erage reversible component. Resolution of the latter is very sensitive to anion adsorption which blocks it but it is also resolved in relative reflectivity measurements.[34] The overall process of surface oxide formation and reduction is represented in Scheme I where the reversible and irreversible stages, which lead to hysteresis, are shown schematically.

This hysteresis in surface oxide formation and reduction plays a major role in the kinetics of electrocatalytic oxidation reactions at Pt and other noble metals, e.g., in oxidation of H_2 and small reactive organic molecules such as HCOOH, CH_3OH, etc. In such reactions, the initial reversibly formed species in the oxide film are reactive while the rearranged state of the film is usually inhibitory. For H_2 oxidation, however, all states of the film at Pt are inhibitory.

Grateful acknowledgment is made to the Natural Sciences and Engineering Research Council, Canada, for support of this and related work.

Infrared Multiphoton Decomposition: Photochemistry and Photophysics

DAVID M. GOLDEN,* MICHEL J. ROSSI, ALAN C. BALDWIN, and JOHN R. BARKER*

Department of Chemical Kinetics, SRI International, Menlo Park, California 94025

Received August 15, 1980

Chemical kineticists often search for experimental tools that allow the preparation and study of molecules with energy distributions other than thermal. Thus, experiments using photochemical and chemical activation are common. Also sought are techniques whereby short-lived species, such as free radicals, may be created under conditions where their reactions may be studied. In this Account, we report on some experiments in which we have employed an infrared laser to achieve both of these results.

In the past 10 years,[1-3] experiments have indicated that polyatomic molecules can be decomposed when subjected to radiation from a high-power infrared laser under conditions where no molecular collisions are possible. Infrared optical pumping is thus a nonthermal energization process.

Three aspects of this phenomenon have been of great interest. First, the molecular decomposition can lead to reactive species, such as free radicals, and thus is a rapid method for preparing such species for chemical and physical study. Second, the optical pumping process may be mode specific, i.e., as many photons are absorbed, they may excite a given molecular vibration to a continually greater degree. This is quite different from collisional excitation which is statistical. Because of this difference, it is conceivable that chemistry induced by laser excitation would be considerably different from that induced by thermal collisional excitation. Finally, since similar molecules with different isotopically substituted molecules absorb infrared radiation of different frequencies, the infrared laser-induced dissociation process is a natural method for isotopic separation. Indeed, these last two points have furnished the major impetus for recent research in this area.

David M. Golden is Director of the Chemical Kinetics Group at SRI International. He was born in New York City in 1935. He received his A.B. degree from Cornell University and the Ph.D. from the University of Minnesota. His research interests are in chemical kinetics, atmospheric chemistry, combustion chemistry, photochemistry, and codification and extrapolation of rate data.

Michel Rossi and Alan Baldwin are Chemists and John Baker is a Senior Chemist at SRI International. Dr. Rossi was born in Germany and studied at the Kollegium Kalksburg in Vienna and at the University of Basel, where he received his Ph.D. in 1975. Dr. Baldwin was born in London, did his undergraduate studies at Imperial College, and received his Ph.D. degree from the University of Leicester in 1976.

Dr. Barker was born in Tennessee and studied at Hampden-Sydney College and then at Carnegie-Mellon University, where he received his Ph.D. in 1969.

Kinetic Model

A model for infrared laser pumping of molecules which has received general acceptance is illustrated in Figure 1. In this particular case, the first two photons are absorbed in a given isolated vibrational mode with the anharmonicity being compensated for by $\Delta J = \pm 1$, leading to allowed transitions. In Figure 1 we depict a situation where the coupling of energy from $v = 2$ of the isolated vibrational mode to the other quantum states of the molecule at this energy is sufficiently strong that we describe the molecule in terms of an energy level, rather than a specific state. At this energy and higher, the density of levels is so great that the resonant absorption of the specific laser photon is assured. This energy region is called the quasicontinuum. Above some barrier to chemical decomposition, a true continuum exists and molecules have lifetimes given by $(k(E))^{-1}$, where $k(E)$ may be computed via RRKM theory or other models for unimolecular decay. The exact nature of pumping in any given molecule is thus strongly dependent on energy-level and wave-function details. If we desire to understand the time history of population in the molecular quantum states, we need to solve the time-dependent Schrödinger equation. It is well-known[4] that under certain conditions the

(1) R. V. Ambartzumian and V. S. Letokhov in "Chemical and Biochemical Applications of Lasers", Vol. 3, C. B. Moore, Ed., Academic Press, New York, 1977.
(2) N. Bloembergen and E. Yablonovitch, *Phys. Today*, **21**, 23 (1978).
(3) P. A. Schultz, Aa. S. Sudbo, D. J. Krajnovich, H. S. Kwok, Y. R. Shen, and Y. T. Lee, *Annu. Rev. Phys. Chem.*, **30**, 379 (1979).

0001-4842/81/0114-0056$01.00/0

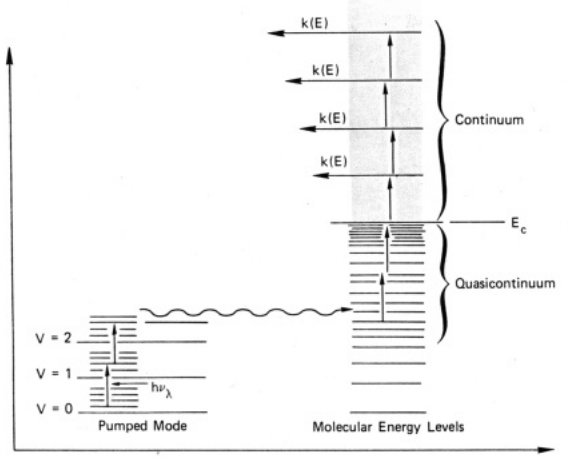

Figure 1. Energy level structure of a polyatomic molecule excited by monochromatic radiation of energy $h\nu_\lambda$.

Schrödinger equation can be approximated by a coupled set of differential rate equations, a "master equation".

Variables at the disposal of researchers include the usual environmental parameters such as temperature and pressure, molecular parameters, such as density of states (entropy), and reaction barrier heights. In addition, there are several laser parameters that may be varied. These include wavelength, intensity (photon flux = photons cm^{-2} s^{-1}), fluence (energy dose = energy cm^{-2}), and the temporal profile of the laser pulse. The properties intensity and power, which is just intensity multiplied by the energy of the photon, are often interchanged. Thus, fluence is the time integral of power and is often written $\phi = \int_0^t I\, dt$.

The question of applicability of master equation representations for infrared multiphoton collisionless decomposition has been extensively treated,[5] and it has been shown that such approaches are applicable here. Thus we write

$$\frac{dN_m}{dt} = C^a_{m-1}N_{m-1} + C^e_m N_{m+1} - (C^a_m + C^e_{m-1} + k_m)N_m \quad (1)$$

to describe the time history of the population of the mth level, where N_m is the population density of level m, C^a_m is the effective first-order rate constant for absorption from level m to $m + 1$, and C^e_m is that for stimulated emission from level $m + 1$ to m. k_m is the rate constant for chemical decomposition from level m and is identically zero if the energy of level m is below the barrier for reaction. Since the level separation is just the photon energy, the numerical solution for this equation is obtained with the natural "grain" size. This is often called an energy-grained master equation (EGME).

The Einstein relation[6] allows us to compute the emission rate constant from the absorption rate constant according to detailed balance:

$$\frac{C^e_m}{C^a_m} = \frac{g_m}{g_{m+1}} \quad (2)$$

where g_m is the molecular density of states at energy $mh\nu$.

The master equation may be an acceptable description of the pumping process for many possible functional forms of the rate constants. We may define an absorption cross section by considering the situation when light of intensity I_0 is incident on a gas sample and induces a molecular transition from level m to $m + 1$. The light intensity is attenuated according to the Beer–Lambert law, $I = I_0 e^{-\sigma_m N_m l}$, where σ_m is the absorption cross section and l is the length of the absorbing gas layer. The effective first-order rate constant for absorption of photons is[6]

$$C^a_m = \frac{\sigma_m I}{h\nu} \quad (3)$$

In this simple case, every term in eq 1 except $k_m N_m$ is linearly dependent on intensity. In general, k_m is small, except for the highest few levels, and thus we see that the decomposition *yield* would depend on fluence. If this description were completely adequate, we could compare experimental yields with ab initio computed yields for determination of the cross section, so we assume a simple power law dependence on internal energy:[7]

$$\sigma_m = \sigma_0(i + 1)^n \quad (4)$$

where σ_0 is the $0 \rightarrow 1$ cross section, i is the number of laser quanta in the molecule, and typically $n < 0$. This reduces the problem to a one-parameter fit. There are two expected complications. First, the cross sections may be intensity dependent in the strong lasr field, and thus rigorous fluence scaling is lost. Second, a molecule might have more than one populated level that interacts with the laser field. If the cross sections are different for each set of pumped levels, we will need an EGME for each. The overall yield will then correspond to a combination of EGMEs. Thus experimental model verification requires the determination of yields as a function of fluence, intensity, and wavelength for molecules with a range of cross sections and densities of states under different conditions of pressure and temperature. This requires a general technique, and we discuss such an experiment in this Account.

Experimental Approach

The need for a universal detector for the study of infrared laser dissociation of polyatomic molecules under collisionless conditions encouraged us to adapt a familiar technique to the study of infrared photochemistry and photophysics. We have been using an experimental technique called very low pressure pyrolysis (VLPP) for a number of years.[8] In this flow technique we use a heated Knudsen cell reactor at low pressures coupled with molecular-beam-sampling mass spectrometric detection to study the gas-phase unimolecular decomposition of organic molecules, and the rapid reactions of subsequently formed free radicals at pressures in the micrometer range and at temperatures from below ambient up to ~1000 °C. We have found this technique to be applicable to the study of unimolecular processes, radical–molecule reactions, radical–radical

(4) W. Pauli, Festschrift Zum 60 Geburtstage, A, Sommerfelds, Hirzel, Leipzig, 1928, as quoted in ref 5.
(5) M. Quack, *J. Chem. Phys.*, **69**, 1282 (1978); *Ber. Bunsenges. Phys. Chem.*, **83**, 757 (1979).
(6) J. I. Steinfeld, "Molecules and Radiation: An Introduction to Modern Molecular Spectroscopy", MIT Press, Cambridge, MA, 1978, pp 24–30.
(7) J. R. Barker, *J. Chem. Phys.*, **72**, 3686 (1980).
(8) S. W. Benson, D. M. Golden, and G. N. Spokes, *Angew. Chem. Int. Ed. Engl.*, **12**, 534 (1973).

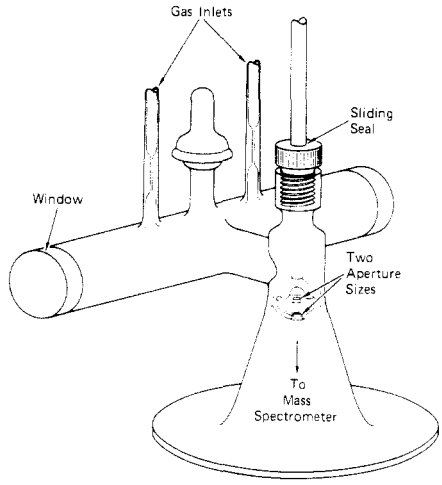

Figure 2. The two-aperture Knudsen cell reactor.

reactions, some equilibrium constants, and catalysis. In some recent work,[9] the general technique has been extended to enable the determination of photoproducts of

$$ClONO_2 \xrightarrow{h\nu} Cl + NO_3$$

irradiated by a Xe arc.

For the work described in this Account, we have modified a VLPP experiment to replace thermal collisional energization with infrared laser energization. We have suitably modified the hardware to collect data in a pulsed rather than steady-state mode.

The basic VLPP molecular-beam-sampling apparatus has been described in detail elsewhere.[8] Briefly, the effusive molecular beam is mechanically chopped in the second (differentially pumped) chamber before it reaches the ionizer of the quadrupole mass filter. The signal is demodulated by a lock-in amplifier whose output is stored in a signal averager (PAR 4202), which also triggers the laser. The two-aperture Knudsen cell (Figure 2) is fitted with KCl windows and has an optical pathlength of 20.5 cm and a volume of approximately 105 cm^3. The cell is coated with Teflon by rinsing with a finely dispersed Teflon slurry in a water/aromatic solvent mixture (Fenton Fluorocarbon, Inc.) and curing at 360 °C. The cell is characterized by the following escape rate constants (two apertures) for a molecule of molecular weight, M, at temperature, T: $k_b = 2.943(T/M)^{1/2}$ s^{-1}, $k_s = 0.883(T/M)^{1/2}$ s^{-1}.

The Lumonics TEA laser (Model K-103) is operated at a pulse repetition frequency of ~0.25 Hz, slow enough to permit >99% of the reaction products to escape from the cell before the next laser shot. The output of the laser consists of a pulse of approximately 6 J, directed through the photolysis cell after being weakly focused by a concave mirror (fl = 10 m), which gives a beam cross section of 2.67 cm^2 at the KCl entrance window of the cell ($1/e^2$-criterion).

Detection of free-radical products by electron-impact mass spectrometry is made difficult by the fact that parent species often have daughter peaks of the same masses as the radical fragments. Thus we have chosen to detect radical species by causing their rapid reaction with a scavenger molecule. Figure 3 shows the signal

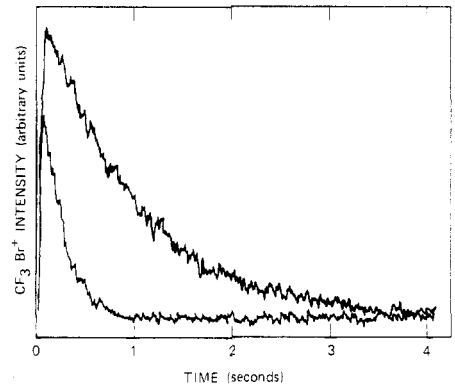

Figure 3. Mass spectrometer signal due to CF_3Br product.

from the CF_3Br product (148/150 amu) arising from the reaction of CF_3 radicals and Br_2. The CF_3 radicals were created from the infrared photolysis of the precursor, CF_3I.[10] The two curves in Figure 3 reflect the two apertures of the reactor.

A typical experiment consisted of averaging the time-dependent mass spectroscopic signal intensity of the products for a number of laser shots (10–100) as a function of the flow rate of the reactant gases at constant precursor flow rate and constant energy per pulse. Although experiments can be performed on a single-shot basis, the signal/noise ratio is improved by averaging the results of a number of laser shots. The total yield of product formed in the reaction of interest is determined by integrating the accumulated time-dependent signal of the signal averager on the strip-chart recorder fitted with an electronic integrator. The signal is calibrated by using known flow rates of products to obtain absolute yields per laser pulse.

Photochemistry

We use the term photochemistry to describe experiments in which laser radiation is used to produce species (usually free radicals) whose thermal rate constants we wish to measure. The modified VLPP technique is well suited for these studies because, regardless of their internal energy upon formation, laser-produced species will collide with the walls of the reactor with a collision frequency of $\sim 10^4$ s^{-1}, thus assuring thermalization (and requiring an awareness of the possibility of heterogeneous reactions).

The following chemical reaction mechanism is appropriate for data interpretation when CF_3 radicals react with Br_2 in our experiments:

$$CF_3I + nh\nu \rightarrow CF_3 + I$$

$$CF_3 + Br_2 \xrightarrow{1} CF_3Br + Br$$

$$CF_3 \xrightarrow{k_w} \text{(wall loss } \textit{not} \text{ yielding } CF_3Br)$$

The secondary reaction of CF_3I + Br is not included because it is too slow at the concentrations of CF_3I used in the present study, and no evidence for it is observed. Similarly, no heterogeneous first-order reaction of CF_3 to produce CF_3Br is included, since the data interpretation does not suggest it. As in the usual data treatment of VLPP studies, each molecular and radical species escapes from the reactor with a characteristic

(9) J. S. Chang, J. R. Barker, J. E. Davenport, and D. M. Golden, *Chem. Phys. Lett.*, **60**, 385 (1979).

(10) M. J. Rossi, J. R. Barker, and D. M. Golden, *J. Chem. Phys.*, **71**, 3722 (1979).

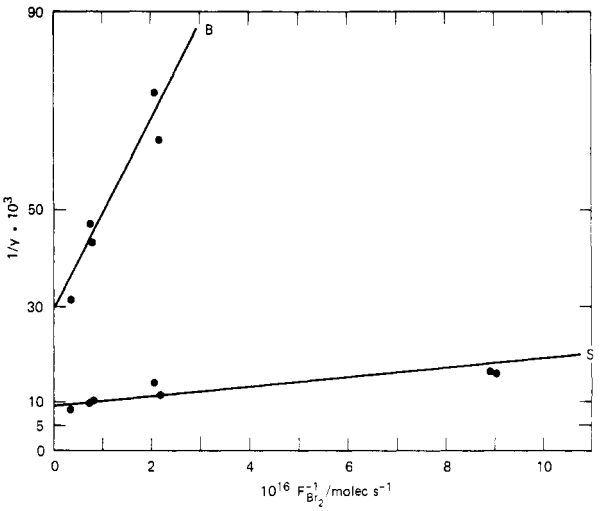

Figure 4. Experimental data for the reaction $C_3F_7 + Br_2 \rightarrow C_3F_7Br + Br$.

first-order escape rate constant; for CF_3I, Br_2, CF_3, and CF_3Br, the escape rate constants are k_2, k_3, k_4, and k_5, respectively.

Analysis of the reaction mechanism and solution of the appropriate differential equations (using LaPlace transforms, for example) give an expression for the time-dependent mass spectrometer signal due to CF_3Br.[10] The total yield of CF_3Br (Y) is related to the rate constants as follows:

$$Y^{-1} = (\alpha\beta V[CF_3I]_0)^{-1}\left[1 + \frac{k_4 + k_w}{k_1[Br_2]}\right]$$

when pseudo-first-order conditions are maintained. In this expression, α is a mass spectrometric sensitivity factor, β is the fraction of the initial CF_3I that is dissociated by the laser pulse, and V is the volume of the cell. The initial $[CF_3I]_0 = F_{CF_3I}/(Vk_2)$, where F_{CF_3I} is the flow rate of CF_3I into the reactor; similarly, $[Br_2] = F_{Br_2}]/(Vk_3)$. For each F_{Br_2}, two escape apertures can be used, giving two different values for the escape rate constants, corresponding to the "big" and "small" apertures, thus creating two independent data sets. Plots of Y^{-1} vs. $F^{-1}_{Br_2}$ give two straight lines with intercepts c_s and c_b (small and big apertures), given by

$$c_i = \frac{k_{2i}}{\alpha\beta V F_{CF_3I}} \qquad i = s, b$$

The slopes of the straight lines are given by

$$m_i = \frac{c_i V(k_4 + k_w)k_{3i}}{k_1}$$

The analytical form remains the same when precursors and "titrants" are changed. Data for CF_3 radicals have been published;[10] Figure 4 shows representative plots for C_3F_7I as precursor for C_3F_7 radicals and Br_2 as titrant.

The rate constants studied in detail up to this time include those in Table I.[10] The reactions of perfluoroalkyl radicals are of some interest, but a reaction of wider interest is

$$t\text{-Bu} + HI \rightarrow i\text{-}C_4H_{10} + I$$

The Arrhenius parameters for this reaction can be combined with those of the reverse reaction to give values for both $\Delta H_f°$ and $S°$ of t-Bu·radical. This reaction is currently under investigation using the molecule $CF_3N{=}N\text{-}t\text{-}C_4H_9$ as precursor.

Table I

reaction	k(300 K)/M^{-1} s^{-1}
$CF_3 + Br_2 \rightarrow CF_3Br + Br$	7.8×10^8
$C_2F_5 + Br_2 \rightarrow C_2F_5Br + Br$	1.8×10^8
$n\text{-}C_3F_7 + Br_2 \rightarrow C_3F_7Br + Br$	2.0×10^8
$CF_3 + NOCl \rightarrow CF_3Cl + NO$	3.5×10^8
$CF_3 + O_3 \rightarrow CF_3O + O_2$	5.6×10^8
$\rightarrow CF_2O + F$	
$CF_3 + NO_2 \rightarrow CF_3O + NO$	1.6×10^9
$\rightarrow CF_2O + F$	

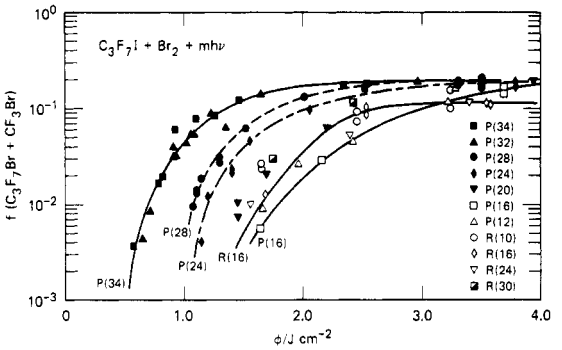

Figure 5. The yield of C_3F_7 from the MPD of C_3F_7I at various wavelengths.

Photophysics

We use the term photophysics to describe the interaction of the laser field and the molecules of interest. For example, the multiphoton decomposition yields depend on the fluence. Indeed, the yield of the MPD process is obtained from integrated areas under curves such as shown in Figures 3 and 4 when the scavenger concentration is sufficient to trap virtually all the radicals. Thus, yields as a function of laser parameters can be obtained in a universal manner. We have studied yields as a function of laser fluences, intensity, and added gas pressure. Results[11] for C_3F_7I at various exciting frequencies are shown in Figure 5. Here the results are displayed as the logarithm of the fraction reacted vs. fluence.

To investigate the assumption that fluence is the most important independent variable, we performed two types of experiments.[12] These experiments take advantage of the fact that the laser output is actually a train of partially mode-locked sharp peaks. If part of the beam is delayed relative to another part, these peaks are split and delayed as depicted in Figure 6. The recombination of the delayed and undelayed beam creates a pulse of the same fluence as the initial beam, but with less intensity, while causing no significant change in the overall pulse envelope. In the simplest experiment, Figure 7a, the transmitted beam is reflected upon itself. By changing the reflecting mirror position with respect to the sample cell, we can vary the instantaneous beam intensity while maintaining a constant fluence. This arrangement has the added advantage that it increases the available fluence by about

(11) M. J. Rossi, J. R. Barker, and D. M. Golden, to be published.
(12) M. J. Rossi, R. Naaman, J. R. Barker, D. M. Golden, and R. N. Zare, to be published.

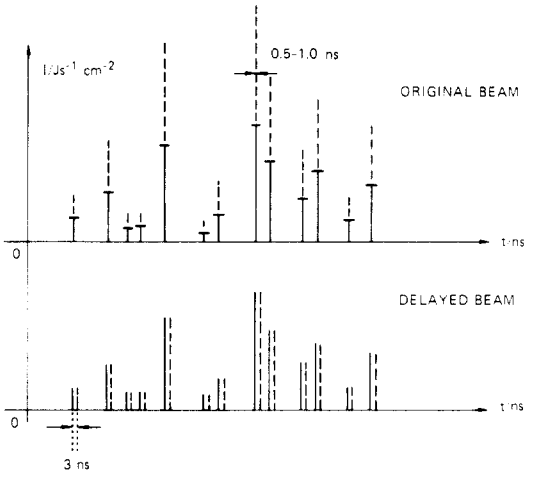

Figure 6. Schematic representation of the experimental intensity profiles.

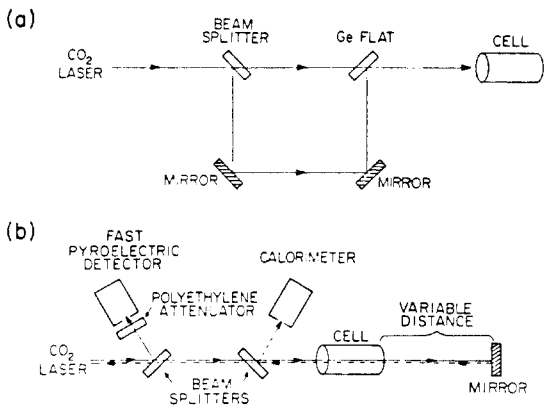

Figure 7. Experimental configuration for varying the intensity at constant fluence.

a factor of 2, and the optical arrangement is simple, although the phase difference between incident and reflected pulses varies over the cell length.

Another method for achieving the same results is the optical delay technique shown in Figure 7b. The pulsed output from the CO_2 laser passes through a beam splitter; one beam is delayed with respect to the other; then the two beams are recombined.

We performed experiments of the first type with both CF_3I and C_3F_7I. The results for the latter, using the method of Figure 7a, are shown in Figure 8. The CF_3I results are similar for both methods of beam delay, illustrating that in both cases intensity effects are clearly observable.

Treatment of Yield Data

In the search for a convenient way to display and analyze data concerning multiphoton yield as a function of fluence, we find[13] that numerical solutions to the EGME over a wide range of physically reasonable parameters (i.e., cross section, density of states, chemical barrier height, and decomposition rate constants) show a regularity that can be used in data interpretation. Typical behavior of the system is shown in Figure 9. After the laser field is turned on, the ensemble of molecules is excited and the average internal energy increases monotonically toward a steady-state level. Figure 9c shows the approach to steady state, defined

(13) A. C. Baldwin and J. R. Barker, *J. Chem. Phys.*, in press.

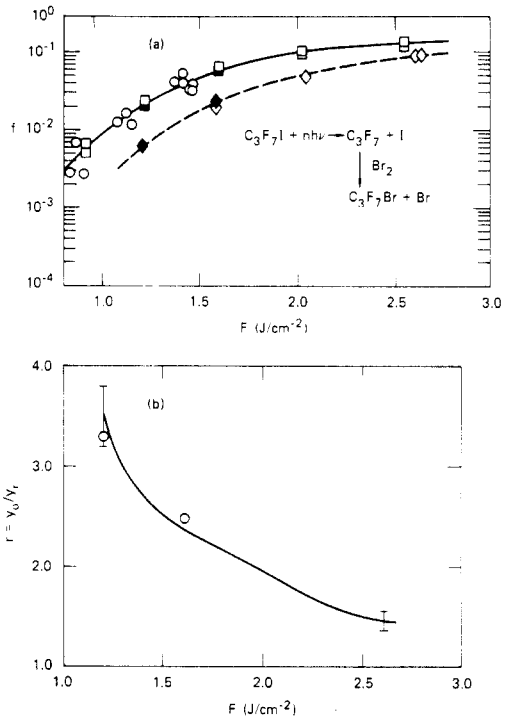

Figure 8. Experimental data on the MPD of C_3F_7I as a function of intensity at constant fluence. (a) (○) Experiments without mirror; (□) experiments with the mirror as close as possible to the sample cell; (◇) experiments with the mirror 30 cm from the cell, causing an average delay of 3 ns with respect to the center of the cell. Filled symbols refer to consecutive experiments in which all conditions remained constant except for the mirror position. (b) The ratio of the results given by the filled symbols in (a).

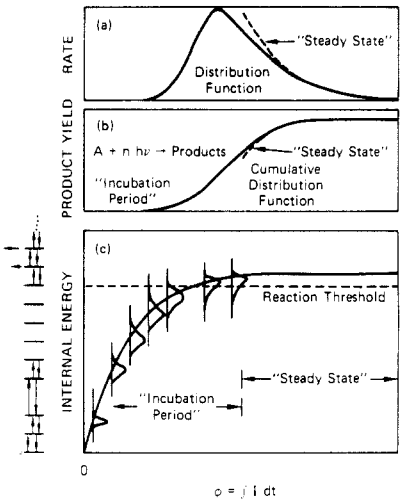

Figure 9. A schematic representation of the behavior predicted by the EGME.

in terms of internal molecular energy, and Figure 9a shows that during this same time the rate of decomposition or the probability that a molecule will decompose in time t to $t + dt$ (i.e., $P(t)dt$) first increases to a maximum and then decays. Figure 9b shows that yield, which is the integral of "rate", is an S-shaped cumulative distribution function (CDF). This CDF represents fractional yield vs. time. The abscissa can be scaled to fluence instead of time by recalling that $\phi = \int_0^t I dt$.

An important discovery is that the distribution function $P(t)$ of reaction times shown in Figure 9a can

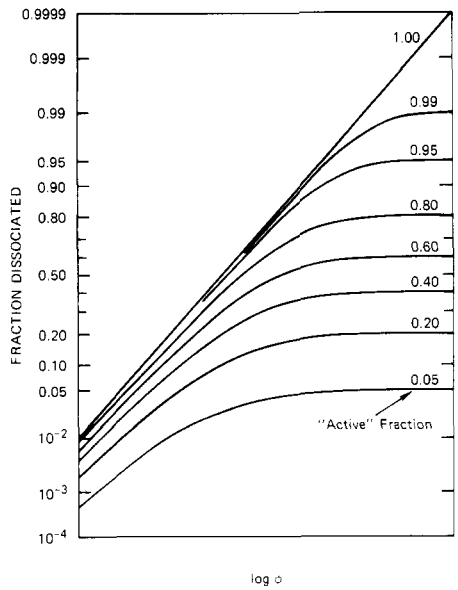

Figure 10. The calculated effect of an inactive population subset on the yield behavior, vs. log fluence.

be represented as a log-normal distribution function (LNDF)[7,13] (μ = mean, σ = standard deviation):

$$P(t) = \frac{1}{\sigma t\sqrt{2\pi}} \exp\left[-\frac{(\ln t - \mu)^2}{2\sigma^2}\right]$$

When the CDF corresponding to this equation is plotted vs. log ϕ (or log t), assuming a time-independent laser intensity, on probability graph paper, the result is a straight line.

This general behavior can also be shown by using the theory of Markovian random walks in finite discrete state space and continuous time.[13] Since the log-normal distribution function is defined by two parameters (μ and σ), we may completely describe the yield behavior of the system by computing analytically the first two moments of the distribution of first passage times of the Markov process without numerically solving the set of differential equations represented by the EGME.[13]

In dealing with real data, several other considerations are important. First, even if an EGME is, in fact, applicable, the spatial profile of the laser must be taken into account. The data shown in Figures 11 and 13 are compared with deconvolutions of this kind. Second, many systems will not exhibit homogeneous behavior, i.e., different groups of molecules will be coupled with the laser field under different conditions (many ladders). A particularly simple version of this effect would be exhibited by a system in which a certain fraction of molecules (active) interact with the laser field, and the rest (inactive) do not. An idealization of such behavior is shown in Figure 10, and a possible example of actual behavior of this type (including spatial profile convolution) from our experiments using the system

$$C_3F_7I \xrightarrow{nh\nu} C_3F_7 + I$$

with C_3F_7 trapped as C_8F_7Br is shown in Figure 11.

If nonhomogeneity involves the coupling of more than one subset of the ensemble of irradiated molecules with the laser field, a linear combination of LNDFs may be required to fit the data. Figure 12 shows some possible results for the subsets in various combinations, and the

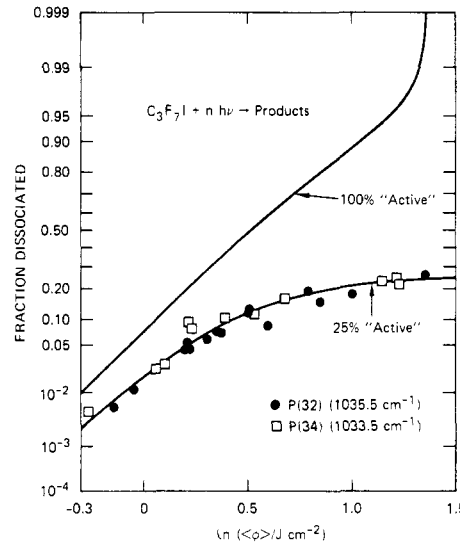

Figure 11. Experimental results (points) for the MPD of C_3F_7I, interpreted in terms of a two-population active/inactive case. The calculated lines have been convoluted with the experimental laser spatial profile.

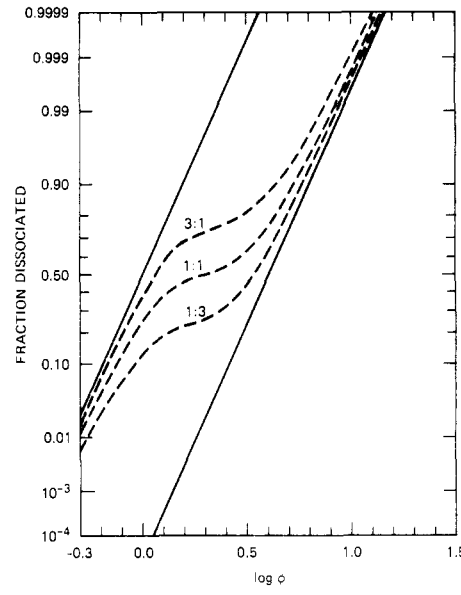

Figure 12. The calculated effect of two active population subsets on the yield behavior, as a function of the relative populations in each subset, plotted on probability graph paper vs. log fluence.

data in Figure 13 labled R(16) gives a possible example of such a two-population case from some of our experiments on CF_3I (CF_3 trapped as CF_3Br). The data in Figure 13 labeled R(8) may be the result of a simple homogeneous case, or a nonhomogeneous case that mimics the simple one.

Energy Transfer

The EGME, which describes a simple incoherently pumped, homogeneously interacting system, is valid only under collisionless conditions. The effects of collisions can be added to the master equation by adding collisional energy transfer rate constants. These rate constants can be described in terms of the parameter $\langle\Delta E\rangle$, the average energy transferred per collision.[14] If, in fact, we have data for the yield vs. fluence under collisionless conditions such that we have arrived at

(14) J. Troe, *J. Chem. Phys.*, **66**, 4745 (1977).

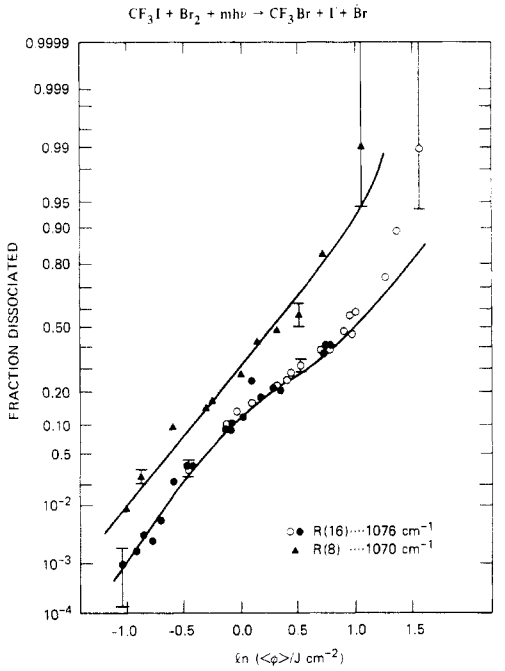

Figure 13. Experimental results (points) for the MPD of CF_3I, interpreted in terms of a simple homogeneous situation R(8) or in terms of two active population subsets, R(16). The calculated lines have been correlated with the experimental laser spatial profile.

suitable values of the absorption cross section and its energy dependence, we may fit the yield as a function of pressure at a given fluence with a value of $\langle \Delta E \rangle$. This value may be compared with values derived from chemical activation (for above threshold) and from low-pressure limit thermal activation (less than or equal to threshold) experiments.

van den Bergh and co-workers[15] have measured the yield of multiphoton decomposition of CF_2HCl as a function of both fluence and pressure of added argon; their data are shown in Figure 14. These data have been simulated as described above,[16] and it was found that a value of $\langle \Delta E \rangle$ of $\sim$0.1 kcal mol^{-1} gives best agreement with the data. Figure 14 shows this fit for three different fluences. (Note that the homogeneous collisionless decomposition fraction is taken from extrapolation to zero pressure.) Introducing collisional terms, which are independent of the laser intensity, into the EGME requires us to consider in detail the exper-

(15) R. Duperrex and H. van den Bergh, *J. Chem. Phys.*, **40**, 275 (1979).
(16) A. C. Baldwin and H. van den Bergh, *J. Chem. Phys.*, in press.

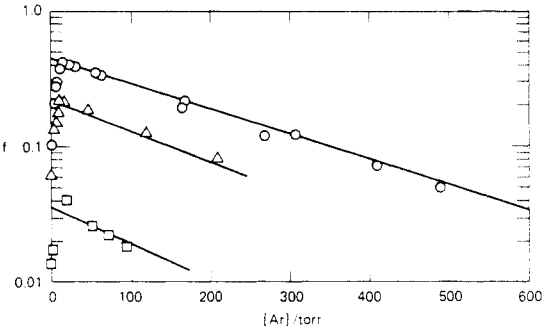

Figure 14. Experimental data (points) on the decomposition of CF_2HCl as a function of fluence and bath gas pressure. The calculated lines are based on an EGME with collisional energy transfer terms included.

imental laser intensity dependence when comparing the EGME predictions with experiment. The good agreement between computed and experimental results in Figure 14 was only obtained by using a parameterized temporal laser intensity profile that approximated the mode-locked spikes of the experimental beam.

Future Directions

We have developed a technique that allows us to extend the experimental range for the determination of rate constants for fundamental processes and at the same time provide data for the detailed physical understanding of the multiphoton decomposition of polyatomic molecules. The photophysical questions raised have occupied much of our effort, but we believe that the photochemical uses of these experimental techniques will prove very interesting and useful to chemists in the long run. We now have the ability to produce reactive species at wall temperatures chosen independently of the production act. Thus, we will be able to extend these rate constant measurements over wide temperature ranges. In addition, we can study average vibrational energy transferred per collision by monitoring the effects of added gases.

A potentially interesting area for future research is the study of branching ratios when more than one reaction pathway exists. Changes in these ratios with laser conditions will be sensitive probes of energy distribution functions and may shed some light on the rate of intramolecular vibrational energy redistribution.

This work was supported by the Air Force Office of Scientific Research, Contract No. F49620-78C-0107. We have benefited from collaboration and discussions with R. N. Zare, J. I. Brauman, and R. Naaman.